RESEARCH ARTICLE

Considering cell viability in 3D printing of structured inks: A comparative and equivalent analysis of fluid forces

Supplementary File

Table S1. Simulation boundary conditions

Location	Boundary condition
Inlet 1, 2, and 3 for 18G needle-related domains	Velocity inlets: a constant value of 2.50 e-5 m/s under normal directional conditions
Inlet 1 for 27G and 32G needle-related domains	Velocity inlets: a constant value of 1.25 e-5 m/s under normal directional conditions
Ink 1	Dynamic viscosity: a constant value of 3.23 Pa·s Density: a constant value of 1030 kg/m³
Ink 2	Dynamic viscosity: a constant value of 3.64 Pa·s Density: a constant value of 1110 kg/m³
Outlet	Pressure outlet: relative pressure at the outlet of 0 Pa
Symmetry	Symmetry planes to replicate the 3D body by mirroring the symmetric 3D models
Wall	No slip shear condition

Table S2. Bisection method for the determination of varying geometric parameters of structured inks for printing vascular-like structures

Varied values of r_1 (mm) (r_2 of 1.155 mm)	3.00	3.05	3.10	3.15	3.20	3.40
Ratio of r_1' to $(0.42 - r_1')$	0.91	0.95	1	1.03	1.07	1.26
Varied values of r_2 (mm) (r_1 of 3.1 mm)	1.140	1.145	1.150	1.155	1.160	1.180
Ratio of r_2' to $(0.42 - r_1' - r_2')$	0.93	0.96	0.99	1	1.03	1.10

Table S3. Bisection method for the determination of varying geometric parameters of structured inks for printing hepatic lobule analogues

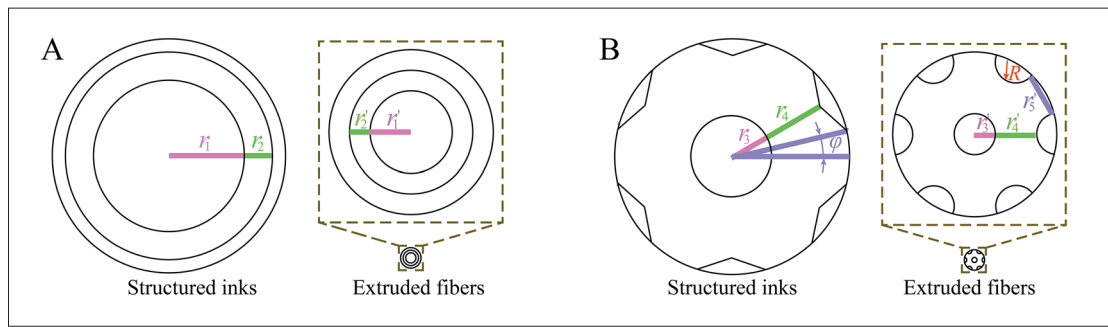| Varied values of r_3 (mm) (r_4 of 2.575 mm and φ of 13.3°)	1.40	1.60	1.65	1.70	1.75	1.80
Ratio of $(0.42 - r_3')$ to r_3'	3.6	3.1	3	2.9	2.8	2.8
Varied values of r_4 (mm) (r_3 of 1.65 mm and φ of 13.3°)	2.560	2.565	2.570	2.575	2.580	2.600
Ratio of r_4' to r_3'	1.92	1.94	1.97	2	2.04	2.15
Varied values of φ (°) (r_3 of 1.65 mm and r_4 of 2.575 mm)	13.0	13.2	13.3	13.4	13.6	13.8
Ratio of r_5' to r_4'	0.97	0.98	1	1.02	1.05	1.09

Figure S1. Cross-sections of two types of structured inks and their corresponding extruded fibers. (A) Vascular-like inks. (B) Hepatic lobule analogue-like inks.
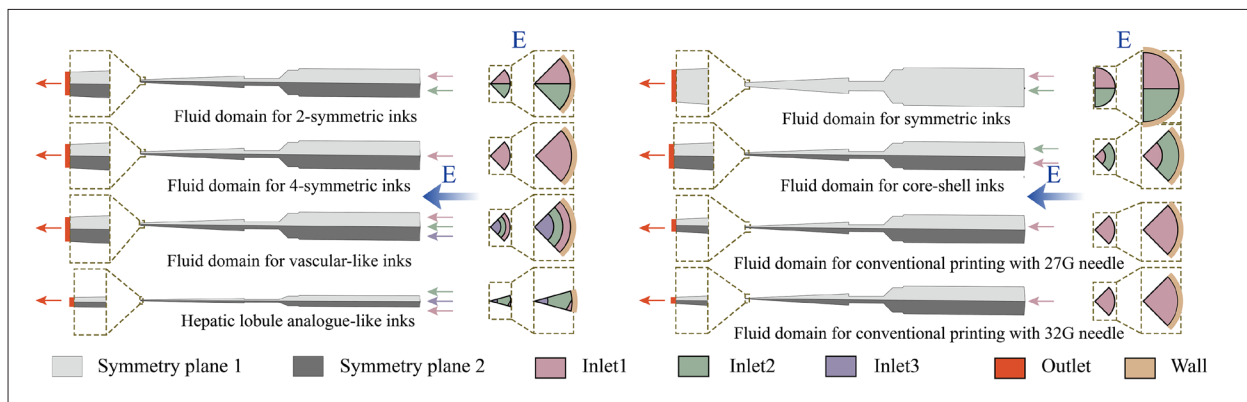

Figure S2. Schematic diagram illustrating boundary conditions for fluid models with various ink types: 2-symmetric inks, 4-symmetric inks, vascular-like inks, hepatic lobule analogue-like inks, symmetric inks, and core-shell inks, for comparative and equivalent analyses.
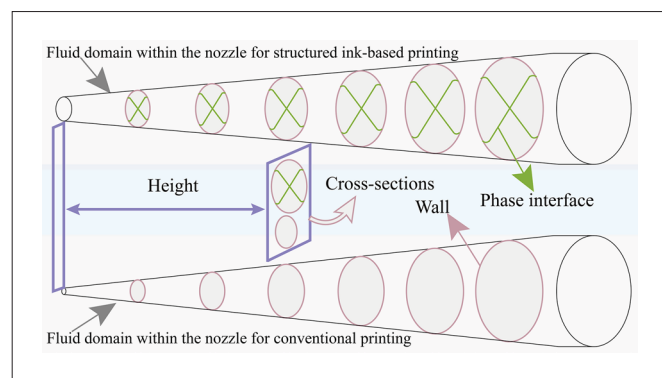

Figure S3. Schematic diagram illustrating cross-sectional positions in the fluid domain within nozzles for structured ink-based printing, and conventional printing, respectively.
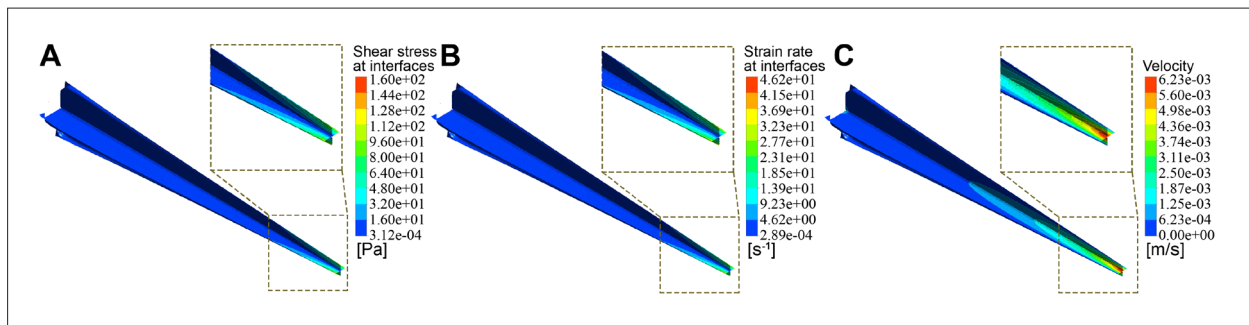
Figure S4. Contour of fluid shear stress, strain rate, and velocity at interfaces in 2-symmetric ink-based printing. (A) Contour of shear stress at interfaces. (B) Contour of strain rate at interfaces. (C) Contour of velocity at interfaces.
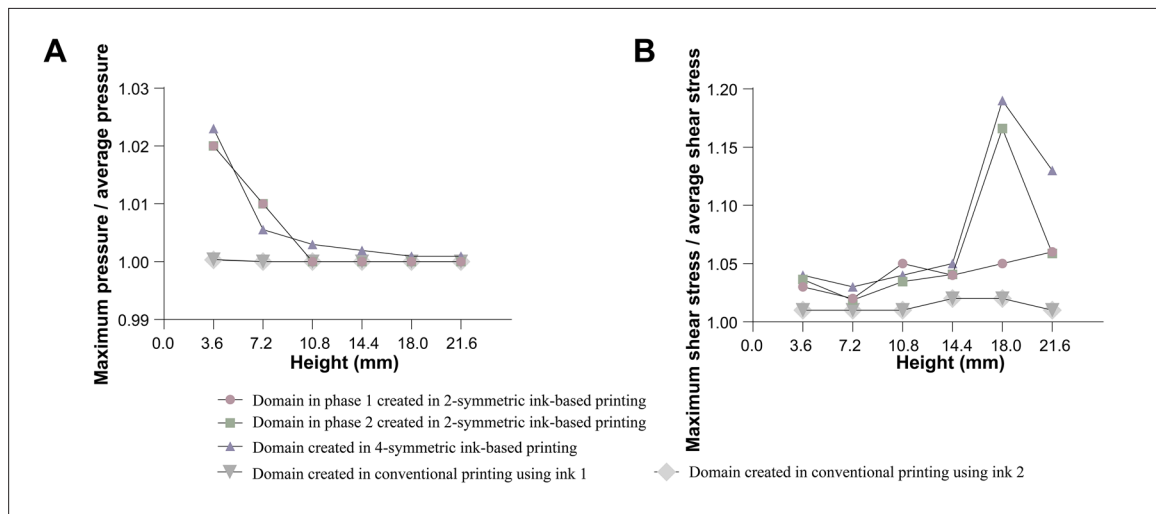

Figure S5. Quantitative analysis of the ratio of fluid maximum pressure to average pressure and the ratio of maximum shear stress to average shear stress. (A) Ratio of maximum pressure to average pressure. (B) Ratio of maximum shear stress to average shear stress.
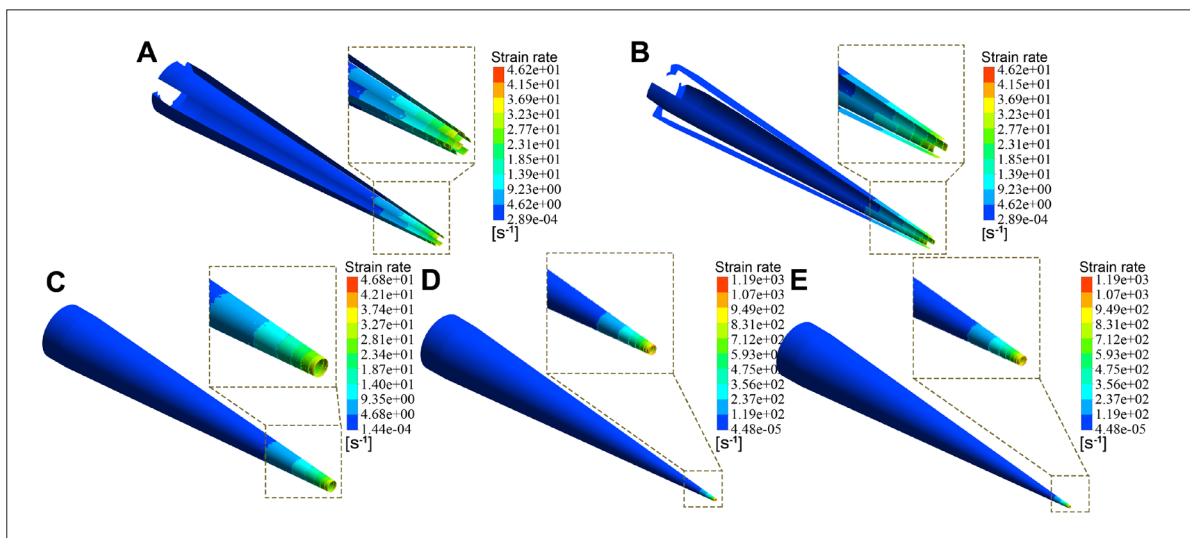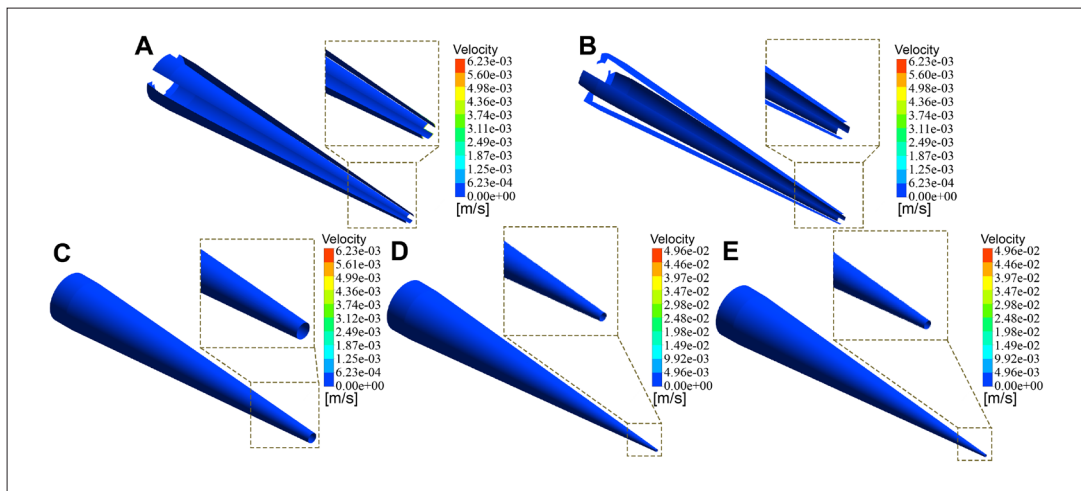

Figure S6. Contour of strain rate for 2-symmetric ink-based printing, 4-symmetric ink-based printing, and corresponding conventional printing. (A) Contour of strain rate of domain in phase 1 in 2-symmetric ink-based printing. (B) Contour of strain rate of domain in phase 2 in 2-symmetric ink-based printing. (C) Contour of strain rate in 4-symmetric ink-based printing. (D) Contour of strain rate in conventional printing using ink 1. (E) Contour of strain rate in conventional printing using ink 2.

Figure S7. Contour of velocity for 2-symmetric ink-based printing, 4-symmetric ink-based printing, and corresponding conventional printing. (A) Contour of velocity of domain in phase 1 in 2-symmetric ink-based printing. (B) Contour of velocity of domain in phase 2 in 2-symmetric ink-based printing. (C) Contour of velocity in 4-symmetric ink-based printing. (D) Contour of velocity in conventional printing using ink 1. (E) Contour of velocity in conventional printing using ink 2.
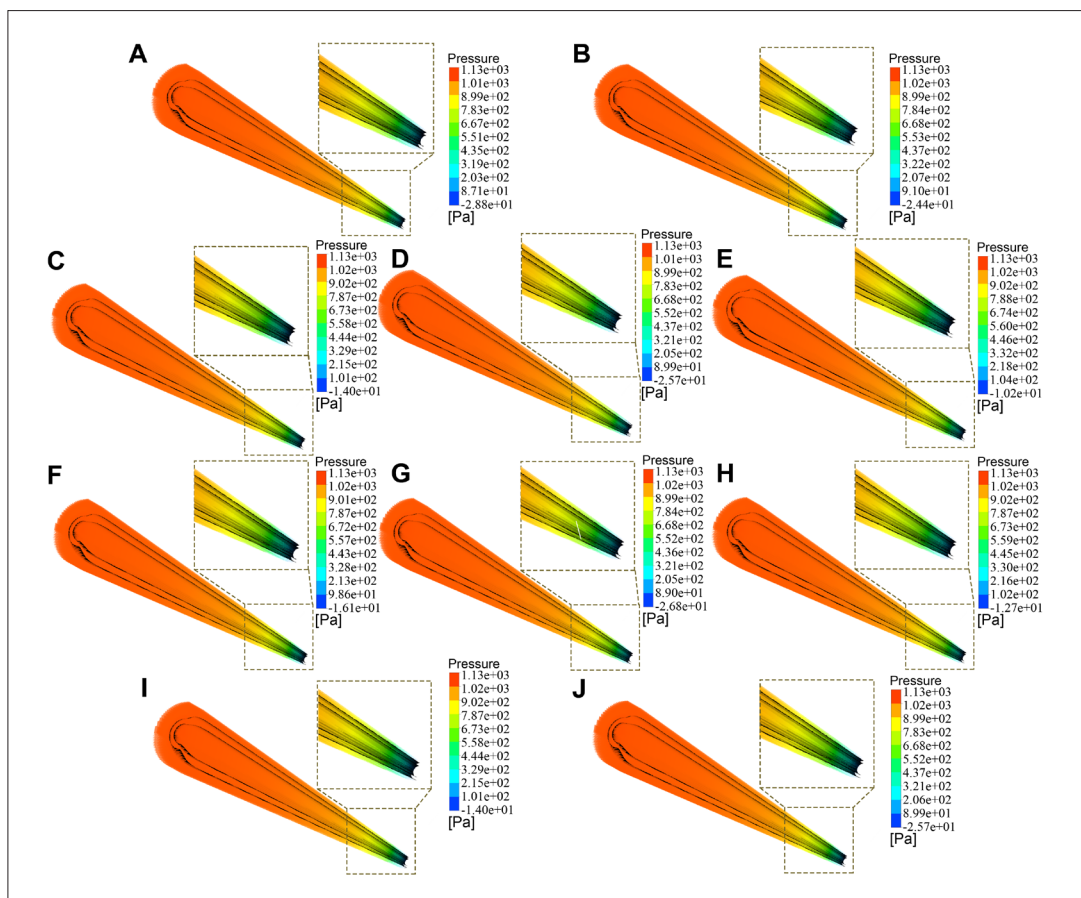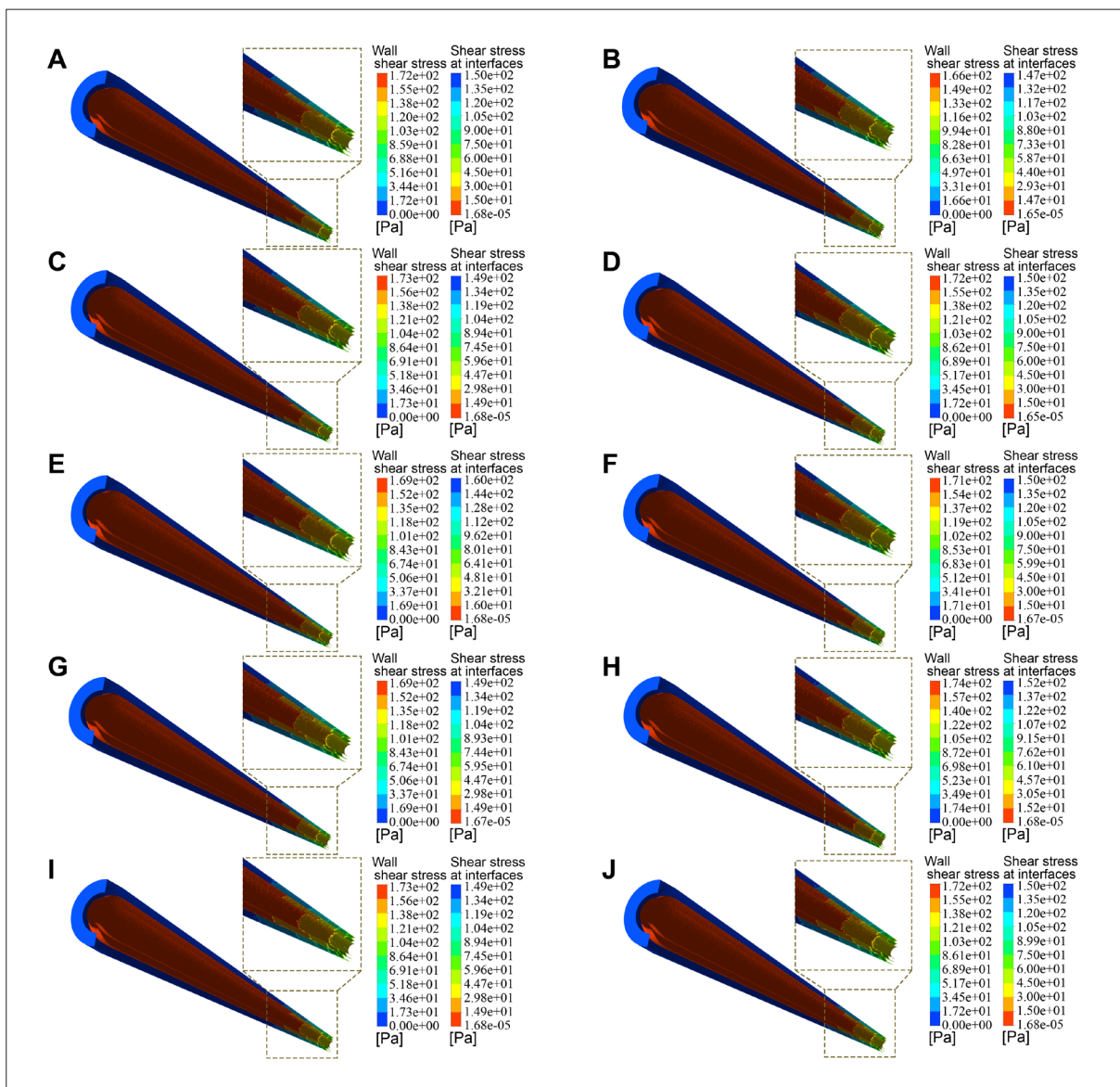

Figure S8. Partial contour of fluid pressure within nozzles in vascular-like ink-based printing using varying values of geometric parameters. (A) Partial contour of pressure with r_1 set to 3.00 mm. (B) Partial contour of pressure with r_1 set to 3.05 mm. (C) Partial contour of pressure with r_1 set to 3.10 mm. (D) Partial contour of pressure with r_1 set to 3.15 mm. (E) Partial contour of pressure with r_1 set to 3.20 mm. (F) Partial contour of pressure with r_2 set to 1.140 mm. (G) Partial contour of pressure with r_2 set to 1.145 mm. (H) Partial contour of pressure with r_2 set to 1.150 mm. (I) Partial contour of pressure with r_2 set to 1.155 mm. (J) Partial contour of pressure with r_2 set to 1.160 mm.
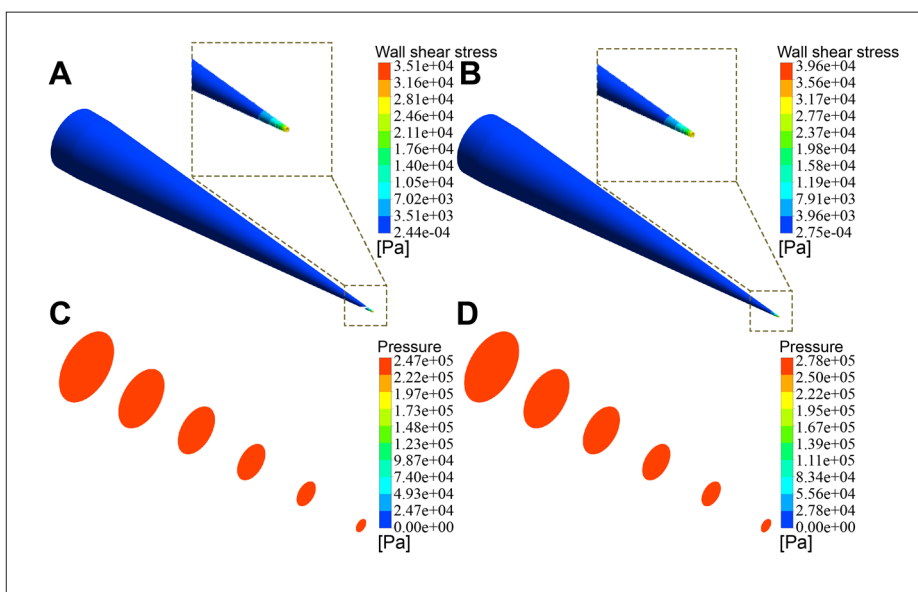
Figure S9. Contour of wall shear stress and pressure in conventional printing with 32G nozzles. (A) Contour of wall shear stress in conventional printing using ink 1. (B) Contour of wall shear stress in conventional printing using ink 2. (C) Contour of pressure in conventional printing using ink 1. (D) Contour of pressure in conventional printing using ink 2.
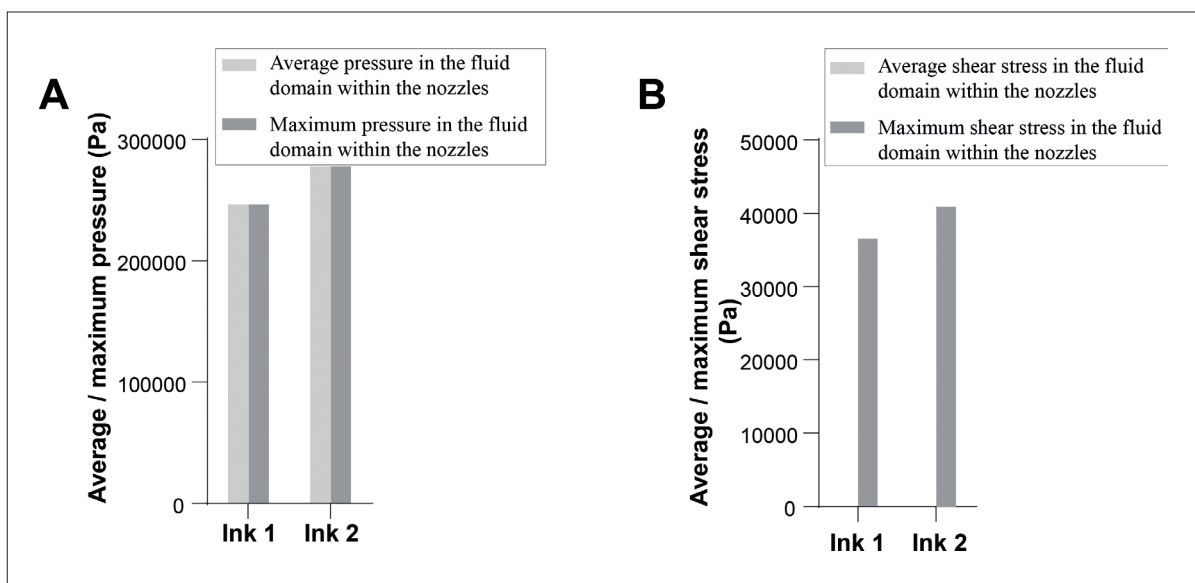
Figure S10. Examination of fluid average pressure, maximum pressure, average shear stress, and maximum shear stress in conventional printing with 32G nozzles. (A) Fluid average and maximum pressure within nozzles with varying inks. (B) Fluid average and maximum shear stress within nozzles with varying inks.

Figure S11. Partial contour of fluid shear stress in the wall and varying material phase interfaces in vascular-like ink-based printing using varying values of geometric parameters. (A) Partial contour of shear stress with r_1 set to 3.00 mm. (B) Partial contour of shear stress with r_1 set to 3.05 mm. (C) Partial contour of shear stress with r_1 set to 3.10 mm. (D) Partial contour of shear stress with r_1 set to 3.15 mm. (E) Partial contour of shear stress with r_1 set to 3.20 mm. (F) Partial contour of shear stress with r_2 set to 1.140 mm. (G) Partial contour of shear stress with r_2 set to 1.145 mm. (H) Partial contour of shear stress with r_2 set to 1.150 mm. (I) Partial contour of shear stress with r_2 set to 1.155 mm. (J) Partial contour of shear stress with r_2 set to 1.160 mm.
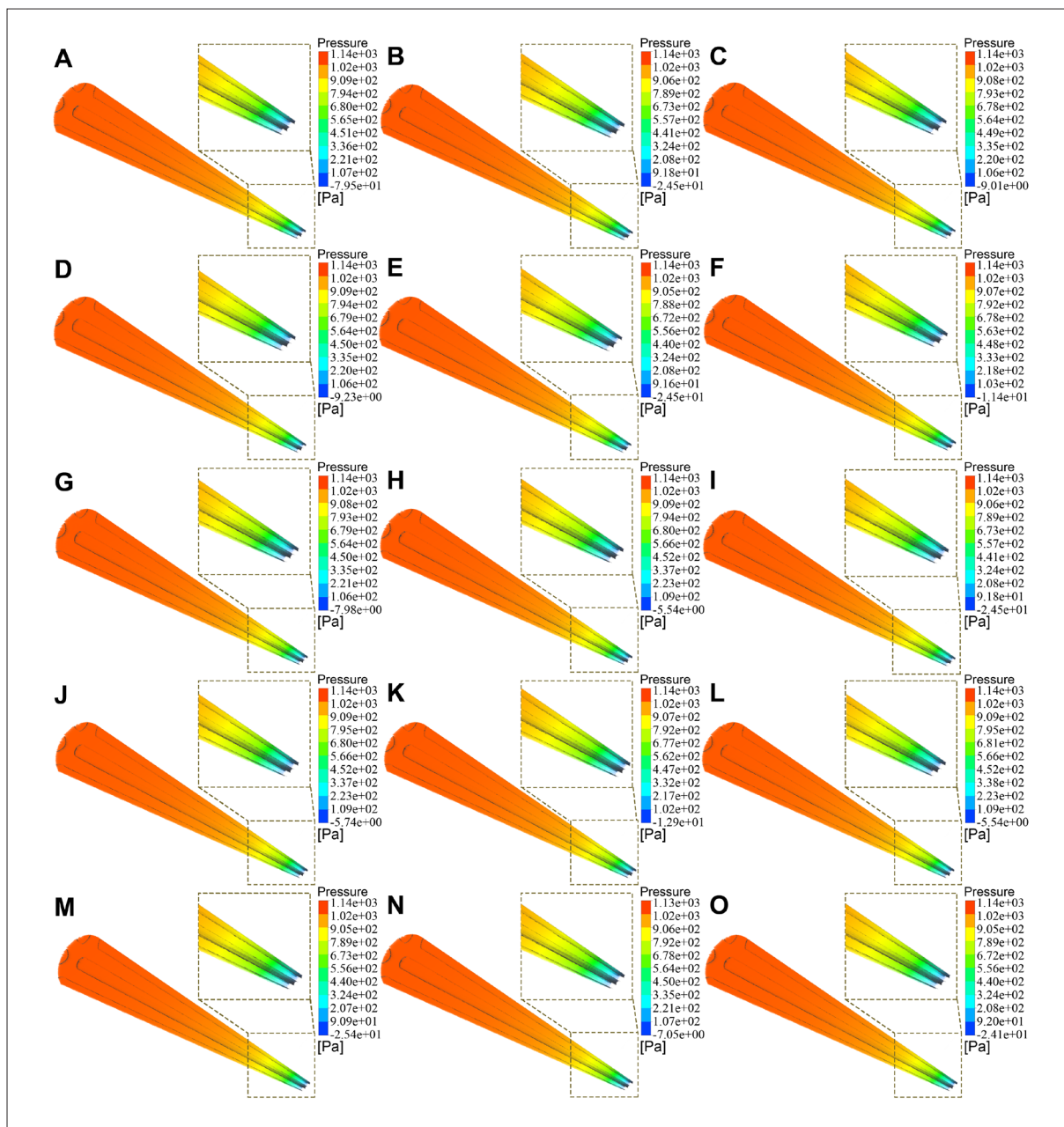
Figure S12. Partial contour of fluid pressure within nozzles in hepatic lobule analogue-like ink-based printing using varying values of geometric parameters. (A) Partial contour of pressure with r_3 set to 1.60 mm. (B) Partial contour of pressure with r_3 set to 1.65 mm. (C) Partial contour of pressure with r_3 set to 1.70 mm. (D) Partial contour of pressure with r_3 set to 1.75 mm. (E) Partial contour of pressure with r_3 set to 1.80 mm. (F) Partial contour of pressure with r_4 set to 2.560 mm. (G) Partial contour of pressure with r_4 set to 2.565 mm. (H) Partial contour of pressure with r_4 set to 2.570 mm. (I) Partial contour of pressure with r_4 set to 2.575 mm. (J) Partial contour of pressure with r_4 set to 2.580 mm. (K) Partial contour of pressure with φ set to 13.0°. (L) Partial contour of pressure with φ set to 13.2°. (M) Partial contour of pressure with φ set to 13.4°. (N) Partial contour of pressure with φ set to 13.6°. (O) Partial contour of pressure with φ set to 13.8°.
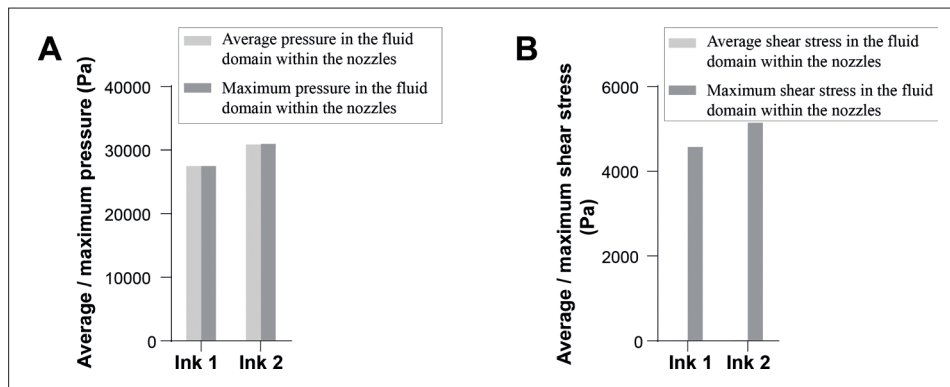
Figure S13. Examination of fluid average pressure, maximum pressure, average shear stress, and maximum shear stress in conventional printing with 27G nozzles. (A) Fluid average and maximum pressure within nozzles with varying inks. (B) Fluid average and maximum shear stress within nozzles with varying inks.
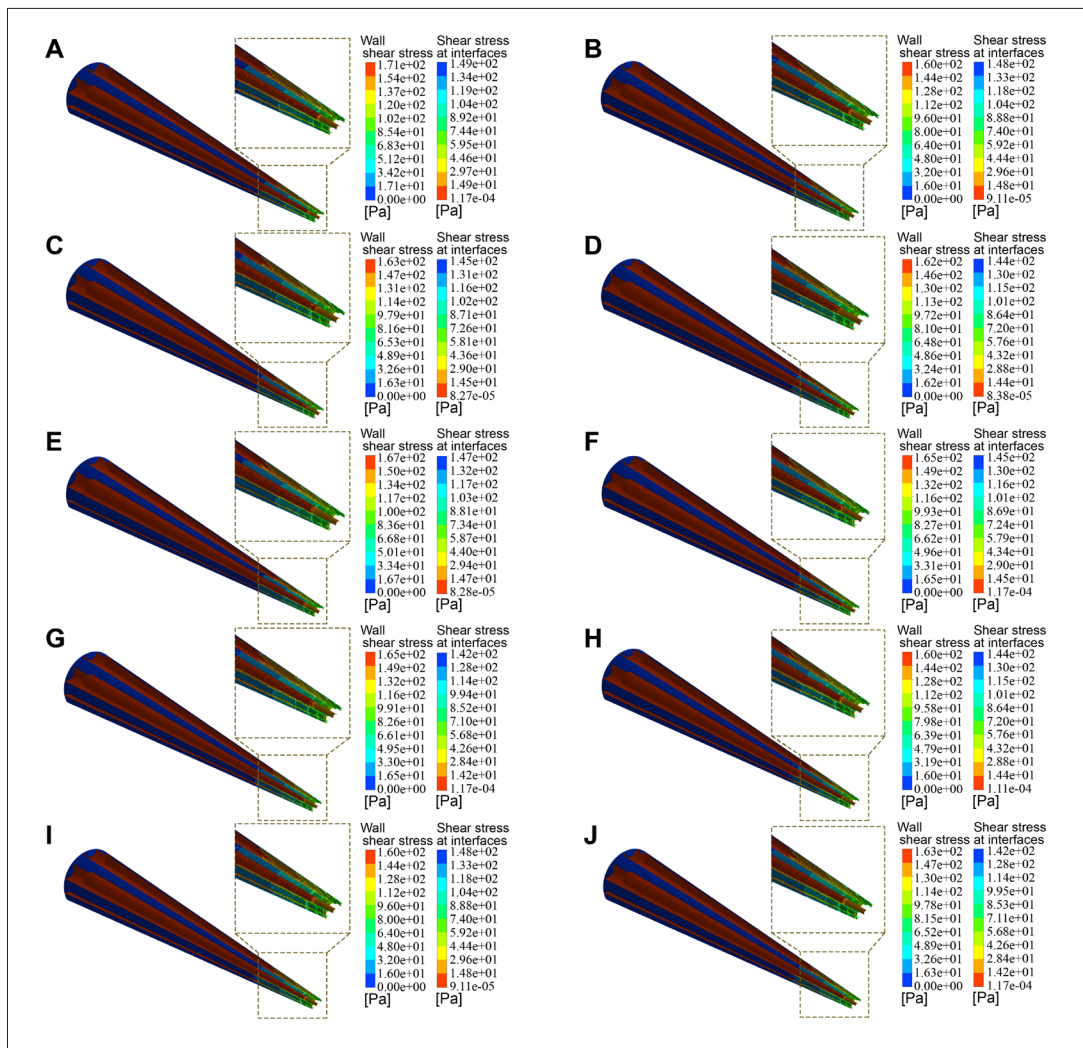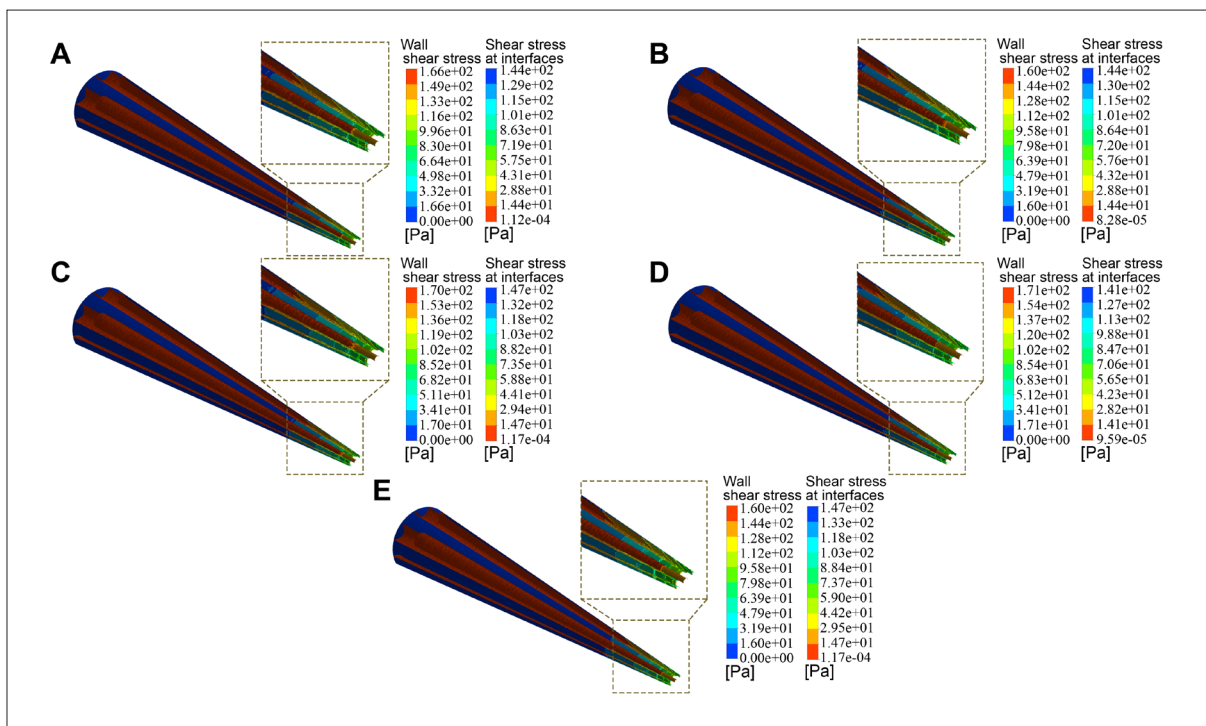

Figure S14. Partial contour of fluid shear stress in the wall and varying material phase interfaces in hepatic lobule analogue-like ink-based printing using varying values of geometric parameter (involving r_3, r_4). (A) Partial contour of shear stress with r_3 set to 1.60 mm. (B) Partial contour of shear stress with r_3 set to 1.65 mm. (C) Partial contour of shear stress with r_3 set to 1.70 mm. (D) Partial contour of shear stress with r_3 set to 1.75 mm. (E) Partial contour of shear stress with r_3 set to 1.80 mm. (F) Partial contour of shear stress with r_4 set to 2.560 mm. (G) Partial contour of shear stress with r_4 set to 2.565 mm. (H) Partial contour of shear stress with r_4 set to 2.570 mm. (I) Partial contour of shear stress with r_4 set to 2.575 mm. (J) Partial contour of shear stress with r_4 set to 2.580 mm.

Figure S15. Partial contour of fluid shear stress in the wall and varying material phase interfaces in hepatic lobule analogue-like ink-based printing using varying values of geometric parameter φ. (A) Partial contour of shear stress with φ set to 13.0°. (B) Partial contour of shear stress with φ set to 13.2°. (C) Partial contour of shear stress with φ set to 13.4°. (D) Partial contour of shear stress with φ set to 13.6°. (E) Partial contour of shear stress with φ set to 13.8°.
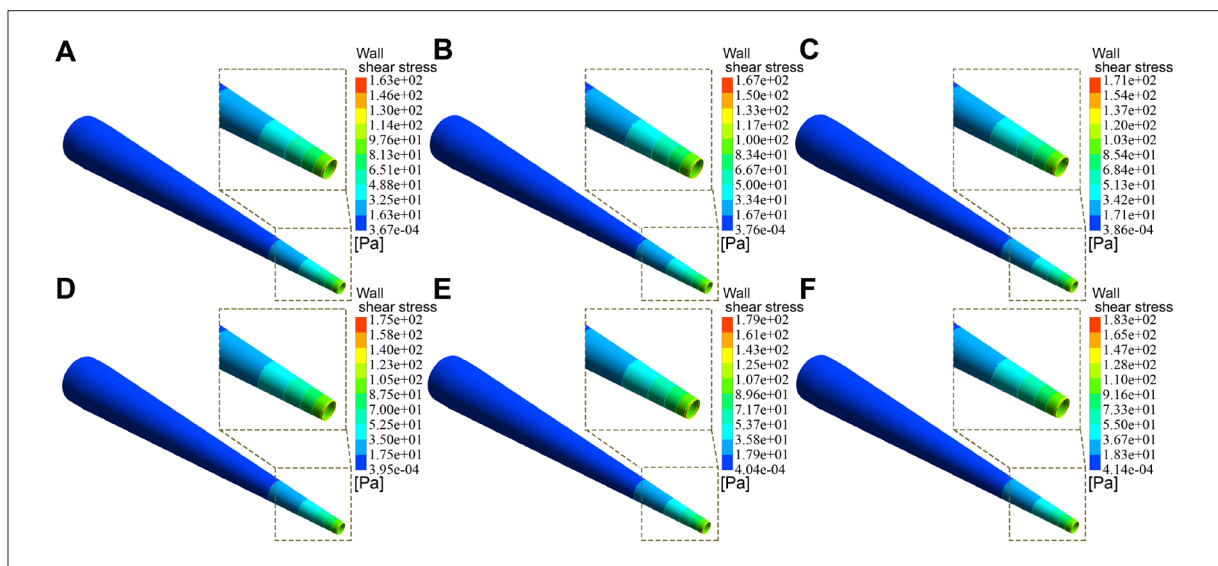
Figure S16. Contour of shear stress of homogeneous inks with varying viscosity for equivalent analysis. (A) Contour of shear stress with viscosity of 3.23 Pa·s and density of 1030 kg/m³. (B) Contour of shear stress with viscosity of 3.312 Pa·s and density of 1030 kg/m³. (C) Contour of shear stress with viscosity of 3.394 Pa·s and density of 1030 kg/m³. (D) Contour of shear stress with viscosity of 3.476 Pa·s and density of 1030 kg/m³. (E) Contour of shear stress with viscosity of 3.558 Pa·s and density of 1030 kg/m³. (F) Contour of shear stress with viscosity of 3.64 Pa·s and density of 1030 kg/m³.
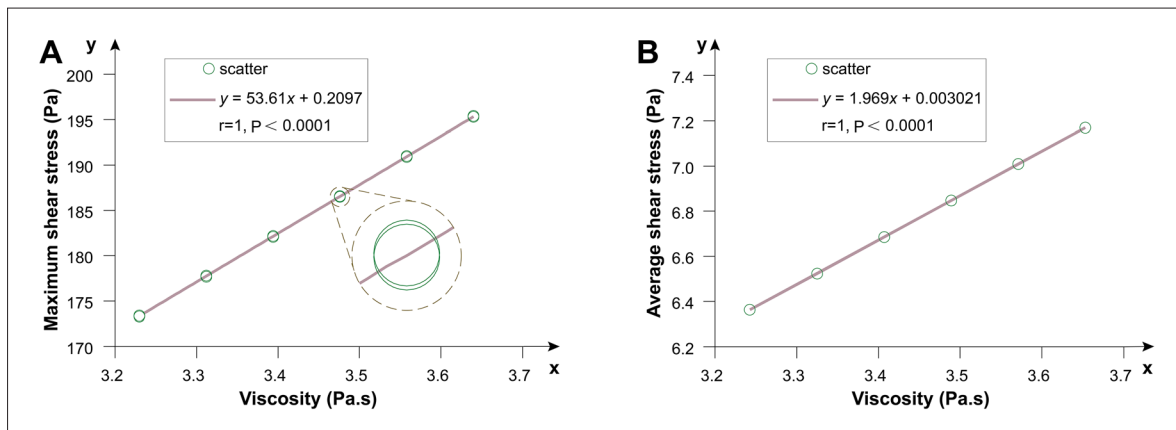
Figure S17. Illustration of the relationship between viscosity and shear stress of homogeneous inks for equivalent analysis. (A) The relationship between viscosity and maximum wall shear stress. (B) The relationship between viscosity and average wall shear stress.
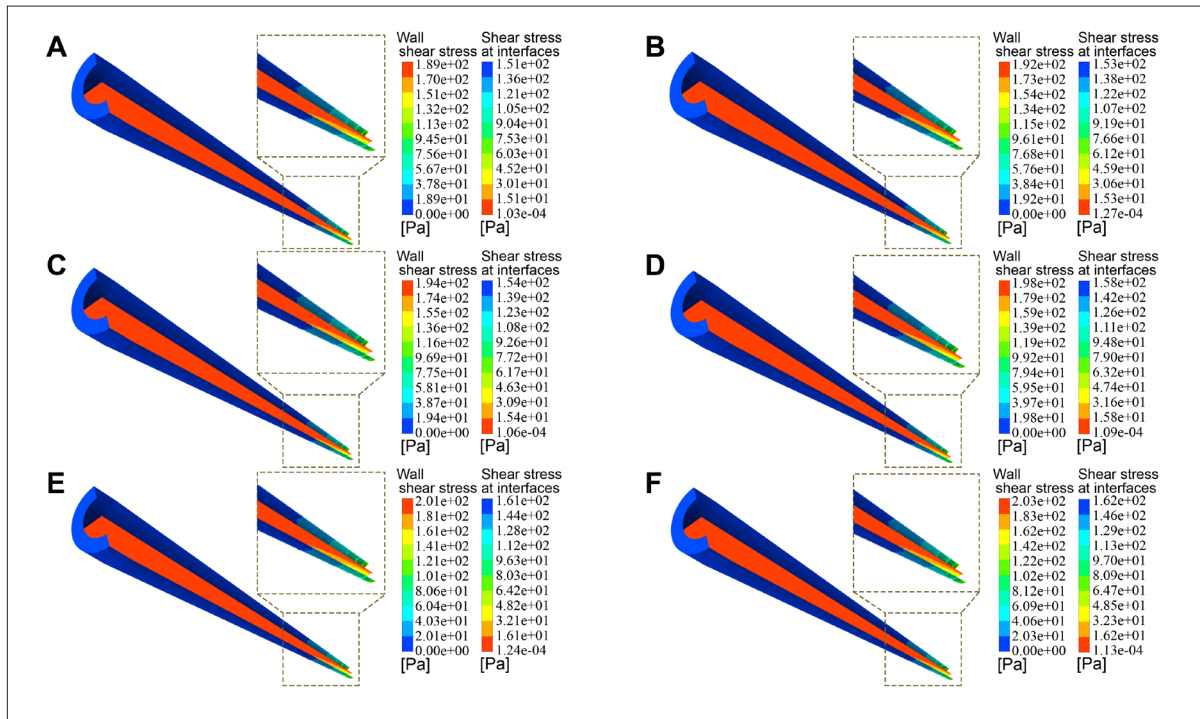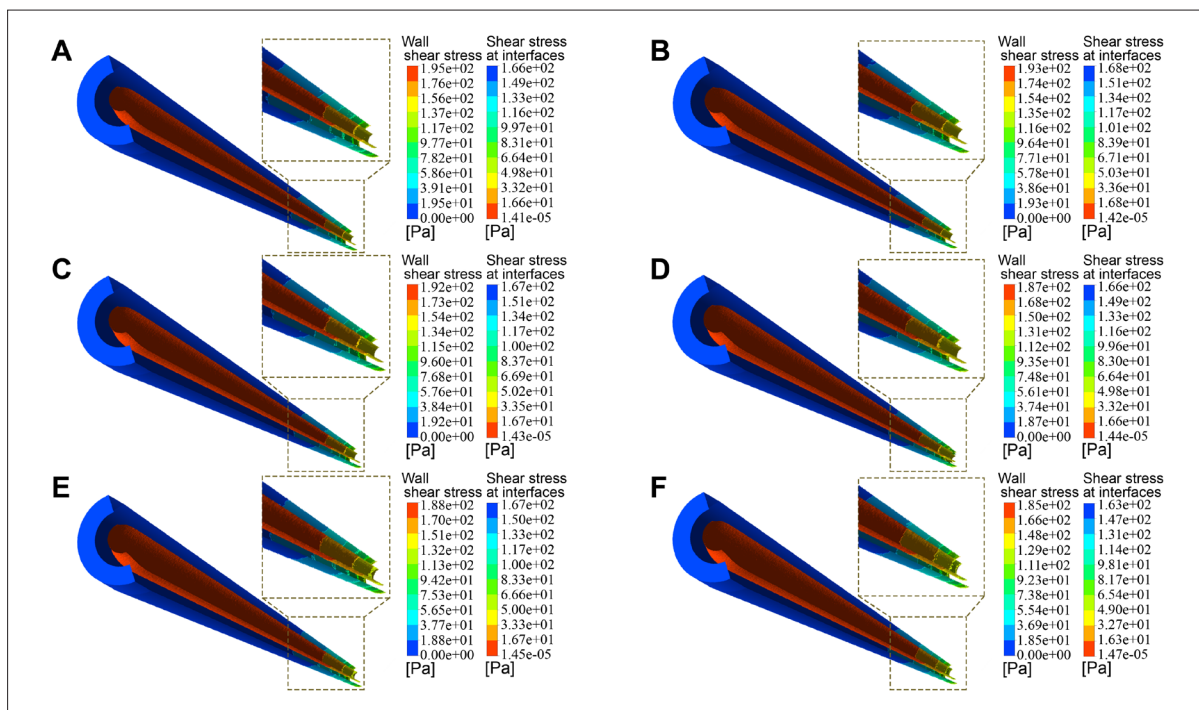

Figure S18. Partial contour of fluid shear stress in the wall and material phase interfaces in symmetric ink-based printing using varying values of ink combinations. (A) Partial contour of shear stress with ink combination of 3.23–3.394. (B) Partial contour of shear stress with ink combination of 3.23–3.476. (C) Partial contour of shear stress with ink combination of 3.312–3.476. (D) Partial contour of shear stress with ink combination of 3.394–3.558. (E) Partial contour of shear stress with ink combination of 3.394–3.64. (F) Partial contour of shear stress with ink combination of 3.476–3.64.

Figure S19. Partial contour of fluid shear stress in the wall and material phase interfaces in core-shell ink-based printing using varying values of core layer radius. (A) Partial contour of shear stress with core layer radius of 2.8 mm. (B) Partial contour of shear stress with core layer radius of 2.9 mm. (C) Partial contour of shear stress with core layer radius of 3.0 mm. (D) Partial contour of shear stress with core layer radius of 3.1 mm. (E) Partial contour of shear stress with core layer radius of 3.2 mm. (F) Partial contour of shear stress with core layer radius of 3.3 mm.
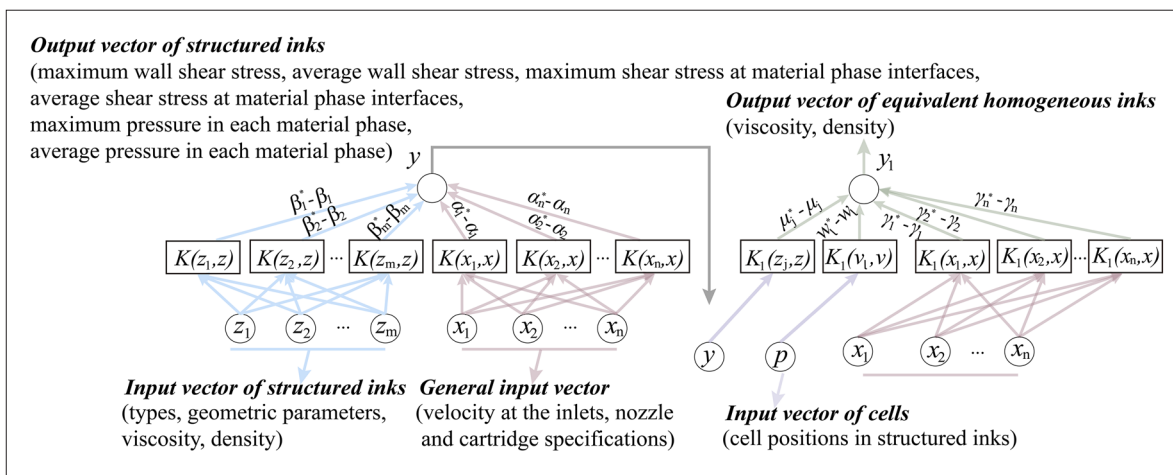
Figure S20. Unraveling fluid forces and equivalent analysis for structured ink-based printing through support vector machine.
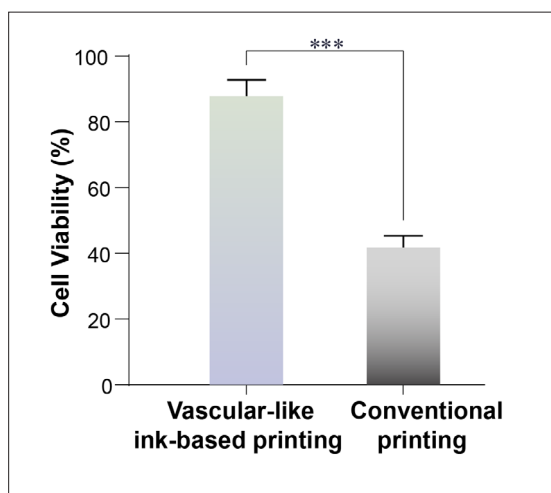
Figure S21. Quantitative comparison of cell viability between fibers printed with vascular-like, cell-loaded outer and intermediary ink layers and those printed via conventional means (***$p < 0.001$).